PHYSICAL REVIEW D **89,** 053011 (2014)

Bounding the Higgs width at the LHC: Complementary results from $H \to WW$

John M. Campbell,[*] and R. Keith Ellis[†]
Fermilab, Batavia, Illinois 60510, USA

Ciaran Williams[‡]
Niels Bohr International Academy and Discovery Center, The Niels Bohr Institute, Blegdamsvej 17, DK-2100 Copenhagen Ø, Denmark

(Received 21 December 2013; published 19 March 2014)

We investigate the potential of the process $gg \to H \to WW$ to provide bounds on the Higgs width. Recent studies using off-shell $H \to ZZ$ events have shown that Run 1 LHC data can constrain the Higgs width, $\Gamma_H < (25\text{–}45)\Gamma_H^{\rm SM}$. Using 20 fb^{-1} of 8 TeV ATLAS data, we estimate a bound on the Higgs boson width from the WW channel between $\Gamma_H < (100\text{–}500)\Gamma_H^{\rm SM}$. The large spread in limits is due to the range of cuts applied in the existing experimental analysis. The stricter cuts designed to search for the on-shell Higgs boson limit the potential number of off-shell events, weakening the constraints. As some of the cuts are lifted, the bounds improve. We show that there is potential in the high transverse mass region to produce upper bounds of the order of $(25\text{–}50)\Gamma_H^{\rm SM}$, depending strongly on the level of systematic uncertainty that can be obtained. Thus, if these systematics can be controlled, a constraint on the Higgs boson width from the $H \to WW$ decay mode can complement a corresponding limit from $H \to ZZ$.

DOI: 10.1103/PhysRevD.89.053011 PACS numbers: 14.80.Bn

I. INTRODUCTION

The discovery of a boson [1,2] that broadly agrees with the predictions of a SM 126 GeV Higgs boson [3–7], represents a tremendous achievement for the LHC experiments and the theoretical predictions of the Standard Model (SM). The continued study of the Higgs boson will provide a detailed understanding of its couplings to the other SM particles. Extraction of these parameters is complicated by the form of the cross section in the narrow width approximation (NWA),

$$\sigma_{i\to H\to f} \sim \frac{g_i^2 g_f^2}{\Gamma_H}. \tag{1}$$

In this approximation the cross section is invariant under the simultaneous rescaling $g_x \to \xi g_x$ and $\Gamma_H \to \xi^4 \Gamma_H$. Therefore attempts to extract coupling information from individual cross section measurements require an assumption of the width, or its direct measurement.

Due to the expected scale of the Higgs width (4 MeV), it is hard to extract its value directly at the LHC because of the inherent detector resolution scale (∼1–2 GeV). Ultimately a precision measurement may be provided by a lepton collider, either by measurement of the invisible Higgs branching ratio (e^+e^-) [8] or a direct threshold scan $(\mu^+\mu^-)$ [9,10]. Until such a time, the LHC can follow a number of alternative strategies that provide less direct constraints. One possibility is to combine experimental results across all Higgs boson production and decay channels [11]. This provides rather stringent limits, $\Gamma_H \lesssim (3\text{–}4)\Gamma_H^{\rm SM}$, albeit with the caveat of mild theoretical assumptions. An alternative approach [12] is to use the mass shift induced by the interference between the Higgs signal and the SM continuum in $H \to \gamma\gamma$ [13–15]. By measuring the mass shift relative to a second channel, one can constrain the couplings and thus the total Higgs width. If the relative mass difference could be measured to $\mathcal{O}(50\text{–}100)$ MeV with 3 ab^{-1} of total LHC data then the upper bound on the width would be $\Gamma_H \lesssim (10\text{–}20)\Gamma_H^{\rm SM}$ [12].

In a recent paper [16] Caola and Melnikov proposed a further mechanism to constrain the Higgs width using the $H \to ZZ \to 4\ell$ decay. The method relies on the fundamental difference between the on-shell cross section shown in Eq. (1) and the off-shell cross section. Away from the resonance region, the Higgs propagator is dominated by the $(s_H - m_H^2)$ term and therefore the number of off-shell Higgs events depends on the coupling rescaling factor ξ. This allows a determination of upper limits on ξ and hence the Higgs boson width. With existing LHC data this method can constrain the Higgs width at the level of $25\Gamma_H$. Potential improvements from kinematic discriminants should sharpen the constraints to around $15\Gamma_H$ [17].

Given its importance it is natural to investigate other channels that may be amenable to a similar analysis. At first glance the lack of mass resolution in the channel $H \to WW \to 2\nu 2\ell$ may appear to undermine the method, which relies on a separation between the peak and off-shell regions. However, the crux of the method relies only on

[*]johnmc@fnal.gov
[†]ellis@fnal.gov
[‡]ciaran@nbi.dk

the existence of this separation and not on its exact reconstruction. Any variable that has well-defined "on" and "off" peak regions can be sensitive to the rescaling parameter ξ. One such variable is the transverse mass M_T [18,19] as adopted in the ATLAS analysis [20],

$$M_T^2 = (E_T^{\rm miss} + E_T^{\ell\ell})^2 - |\mathbf{p}_T^{\ell\ell} + \mathbf{E}_T^{\rm miss}|^2, \qquad (2)$$

where $E_T^{\ell\ell} = (|\mathbf{p}_T^{\ell\ell}|^2 + m_{\ell\ell}^2)^{1/2}$. We note that at LO in perturbation theory (for WW final states) the second term in M_T is identically zero. As such the on-shell events necessarily have $M_T < m_H$, resulting in a prominent edge in the distribution. For the off-shell events no such restriction applies. Therefore a comparison of the cross sections in the two regions $M_T < m_H$ and $M_T > m_H$ provides information on the Higgs boson width.

The WW channel has several advantages when compared to the ZZ decay. Firstly, the threshold for producing two real W bosons is much closer than the threshold for two Z bosons. Secondly the branching ratio into the leptonic final state is much larger. Combined, this means that the number of Higgs events is about two orders of magnitude larger since $\mathrm{Br}(H \to WW) \times \mathrm{Br}(W \to \ell\nu)^2 = 2.7 \times 10^{-3}$ while $\mathrm{Br}(H \to ZZ) \times \mathrm{Br}(Z \to \ell^+\ell^-)^2 = 3.2 \times 10^{-5}$. On the other hand this channel has several disadvantages. The primary concern is that it suffers from a more extensive list of backgrounds that are both larger and more complicated to remove than in the ZZ analysis. The top background is overwhelming in the inclusive sample but a jet veto can be used to isolate Higgs bosons produced through gluon fusion. Using the 7 and 8 TeV data ATLAS [20] and CMS [21] have found evidence for a 126 GeV Higgs boson in this channel with a significance of 3.8 and 3.1 standard deviations, respectively. Very recently CMS have updated their results to include the full 8 TeV data set, improving the significance to 4.3 standard deviations [22].

In this paper we apply the technique of Ref. [16] to the WW channel, and investigate its potential to bound the Higgs width at the LHC. In Sec. II we briefly describe our calculations and present our results for the off-shell cross section as a function of the Higgs width rescaling. Section III uses recent results from ATLAS to bound the Higgs width and discusses future improvements that could be made to facilitate a stronger bound. Finally we draw our conclusions in Sec. IV.

II. RESULTS

In order to correctly model the off-shell spectrum it is crucial to include the effects of the interference between the SM continuum and the Higgs production of WW. The SM continuum proceeds through a gluon-induced loop of fermions. This process has a rich history, with the first calculations performed (for on-shell W bosons) in the late 1980s [23,24]. Off-shell effects, including vector boson decays were presented in [25] and updated to include the full mass of the top and bottom quarks in [26]. Full analytic results for helicity amplitudes with massless quarks were presented in Ref. [27], which made use of the $e^+e^- \to 4$ parton amplitudes of Ref. [28]. These results were extended to include the mass of the top quark in [29] and a detailed study of the effect on the Higgs interference (for searches over a wide range of Higgs masses) was presented. More recently the interference has been studied in the context of a 125 GeV Higgs boson [30,31]. Higher-order corrections to the interference, computed using a soft-collinear approximation to NLO and NNLO, have been investigated in ref [32].

In this paper we use the implementation of $\nu_e e^+ \mu^- \bar{\nu}_\mu$ production in the parton level integrator MCFM 6.7. This includes the effect of massive top and bottom quarks in the Higgs amplitude, while the continuum amplitude accounts for the effect of the top quark mass while leaving the b-quarks massless. Our electroweak parameters are listed in Table I and correspond to the default choices in MCFM. For definiteness in this section we will only present cross sections and distributions for the combination $e^+\mu^-$; the results would be identical for $e^-\mu^+$. In this paper we do not consider the e^+e^- or $\mu^+\mu^-$ final states, which require stricter phase space selection criteria to suppress the Z contributions.

We will present results for a set of cuts designed to mimic the analysis reported by the ATLAS collaboration in Ref. [20]. A list of the cuts that we apply is given in Table II ("full" cuts). The number of off-shell Higgs events is particularly sensitive to two of these cuts, namely those on the dilepton invariant mass $m_{\ell\ell}$, and the azimuthal angle $\phi_{\ell\ell}$. These are subject to the upper bounds,

$$m_{\ell\ell} < 50 \text{ GeV}, \qquad \Delta\phi_{\ell\ell} < 1.8. \qquad (3)$$

In order to regain sensitivity to the off-shell region we will also consider the scenario in which the above dilepton

TABLE I. Mass, width and electroweak parameters used to produce the results in this paper.

m_H	126 GeV	Γ_H	0.004307 GeV
m_W	80.398 GeV	Γ_W	2.1054 GeV
m_t	173.2 GeV	m_b	4.75 GeV
e^2	0.0949563	g_W^2	0.4264904
$\sin^2\theta_W$	0.2226459	G_F	0.116639×10^{-4}

TABLE II. The cuts used in this paper, referred to as "full" cuts, designed to mimic the $e\mu + \mu e$ analysis of ATLAS [20].

$\lvert\eta_e\rvert < 2.47$ excluding $1.37 < \lvert\eta_e\rvert < 1.52$	
$\lvert\eta_\mu\rvert < 2.5$	$10 \text{ GeV} < m_{\ell\ell} < 50 \text{ GeV}$
$p_T^e(\text{hardest}) > 25$ GeV	$\Delta\phi_{\ell\ell} < 1.8$
$p_T^e(\text{softest}) > 15$ GeV	$E_{T,\rm miss}^{\rm rel} > 25$ GeV
$p_T^{\ell\ell} > 30$ GeV	$\lvert\Delta\phi_{\ell\ell,\rm MET}\rvert > \pi/2$

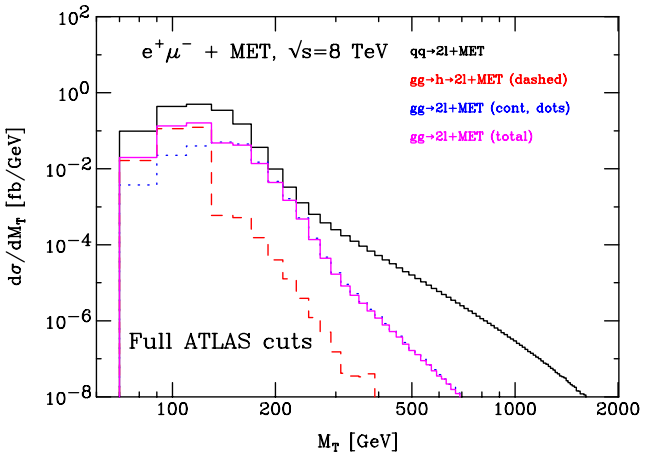

FIG. 1 (color online). Overall picture at 8 TeV (color online), with the full ATLAS cuts described in Table II imposed. The black (heavy solid) line represents the $q\bar{q}$ LO prediction, while the magenta (light solid) line represents the total gg contribution. The red (dashed) line indicates the gg contribution mediated by Higgs boson exchange while the blue (dotted) line shows the gg continuum contribution.

invariant mass cut is removed and the case in which both of these cuts are removed ("basic" cuts).

We present the contribution of the Higgs signal and gluon-gluon box diagrams, together with the dominant $q\bar{q} \to W^+W^- \to e^+\mu^-\nu_e\bar{\nu}_\mu$ background process, in Figs. 1 and 2. Results are shown as a function of the transverse mass M_T defined in Eq. (2), for $m_H = 126$ GeV at $\sqrt{s} = 8$ TeV and for the decay of the W^+ into an electron and W^- into a muon. The renormalization and factorization scales are set equal to $\hat{s}/2$, where $\sqrt{\hat{s}}$ is the partonic center-of-mass energy. Note that, in our calculations, $\hat{s}$ is identical to the four-momentum squared of the final state. Figs. 1 and 2 contain a mixture of orders in perturbation theory. The $q\bar{q}$ process is included at lowest order in perturbation theory $O(g_W^8)$, whereas the other processes are included at $O(g_W^8 g_s^4)$; i.e., they are next-to-next-to leading with respect to the $q\bar{q}$ process, but enhanced by large gluon fluxes at the LHC. The kinematic edge at the Higgs boson mass is visible. At high values of M_T, and hence of $\sqrt{\hat{s}}$, the effect of the interference is destructive and cancels the leading high energy behavior of the $gg \to W^+W^- \to 2\ell 2\nu$ process. Comparing Figs. 1 and 2 it is clear that the full ATLAS cuts greatly reduce the impact of the off-peak region. We note that one way of mitigating this suppression in the future might be to apply only the $\Delta\phi_{\ell\ell}$ cut in Eq. (3), removing the upper bound on the dilepton invariant mass. As can be seen from Fig. 3, this has the advantage of maintaining a strong rejection of the continuum background while accepting more of the high-M_T tail.

Table III shows the cross section in bins of transverse mass, corresponding to the Higgs peak region $M_T <$ 130 GeV and in two off-shell regions defined by $M_T >$ 130 and $M_T > 300$ GeV. In this table the cross sections correspond to the following matrix elements,

$$\sigma^H : |\mathcal{M}_H|^2, \qquad \sigma^I : |\mathcal{M}_H + \mathcal{M}_C|^2 - |\mathcal{M}_C|^2 - |\mathcal{M}_H|^2, \tag{4}$$

where $\mathcal{M}_H$ is the Higgs production amplitude and $\mathcal{M}_C$ is the amplitude for the continuum background. Assuming the

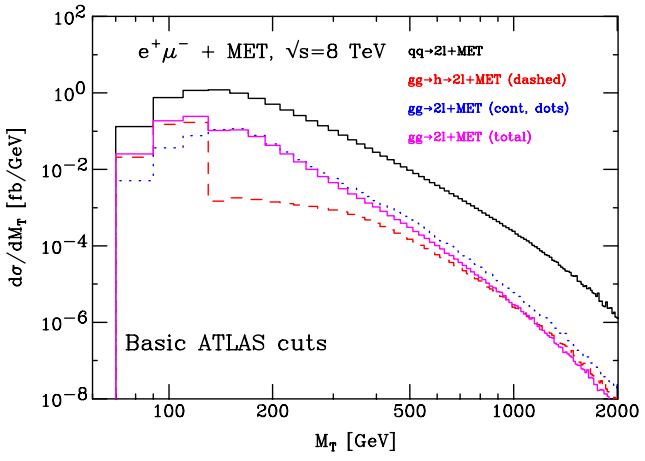

FIG. 2 (color online). Overall picture at 8 TeV (color online), under the basic ATLAS cuts, i.e., when neither the $m_{\ell\ell}$ nor the $\Delta\phi_{\ell\ell}$ cut in Eq. (3) has been applied. The black (heavy solid) line represents the $q\bar{q}$ LO prediction, while the magenta (light solid) line represents the total gg contribution. The red (dashed) line indicates the gg contribution mediated by Higgs boson exchange while the blue (dotted) line shows the gg continuum contribution.

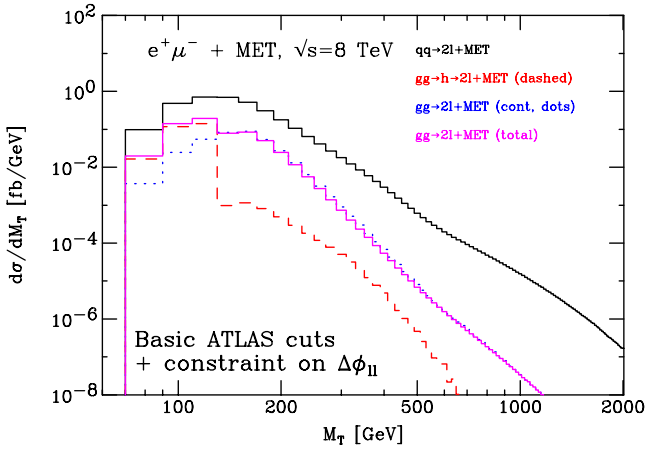

FIG. 3 (color online). Overall picture at 8 TeV (color online). In this figure the ATLAS cuts described in the text have been imposed, including the $\Delta\phi_{\ell\ell}$ cut in Eq. (3) but removing the constraint on the maximum invariant mass of the dilepton pair. The black (heavy solid) line represents the $q\bar{q}$ LO prediction, while the magenta (light solid) line represents the total gg contribution. The red (dashed) line indicates the gg contribution mediated by Higgs boson exchange while the blue (dotted) line shows the gg continuum contribution.

TABLE III. Fiducial cross sections for $pp \to W^+W^- \to \nu_e e^+ \mu^- \bar{\nu}_\mu$ in fb, for the LHC operating at $\sqrt{s} = 8$ TeV. All cross sections are computed with leading-order MSTW 2008 parton distribution functions [33] and renormalization and factorization scales set equal to $\hat{s}/2$.

	$M_T < 130$ GeV		$M_T > 130$ GeV		$M_T > 300$ GeV	
Cuts	σ^H	σ^I	σ^H	σ^I	σ^H	σ^I
Full	5.06	−0.0778	0.0262	−0.173	...	...
basic + $\Delta\phi_{\ell\ell}$	5.52	−0.0924	0.0844	−0.483	0.0021	−0.00888
Basic	6.85	−0.117	0.328	−1.07	0.104	−0.240

TABLE IV. The $q\bar{q} \to W^+W^- \to \nu_e e^+ \mu^- \bar{\nu}_\mu$ background at $\sqrt{s} = 8$ TeV (in fb) calculated for the transverse mass ranges of interest and the three regimes of cuts described in the text.

$\sigma^{q\bar{q}}$	$M_T < 130$ GeV	$M_T > 130$ GeV	$M_T > 300$ GeV
Full	20.6	11.1	0.0171
basic + $\Delta\phi_{\ell\ell}$	25.8	39.9	1.02
Basic	41.2	97.1	8.48

TABLE V. The same as Table III but at $\sqrt{s} = 13$ TeV.

	$M_T < 130$ GeV		$M_T > 130$ GeV		$M_T > 300$ GeV	
Cuts	σ^H	σ^I	σ^H	σ^I	σ^H	σ^I
Full	11.3	−0.195	0.0658	−0.431	...	−0.000185
basic + $\Delta\phi_{\ell\ell}$	12.3	−0.233	0.222	−1.25	0.00698	−0.0283
Basic	15.2	−0.296	1.04	−3.15	0.393	−0.893

Standard Model width for the Higgs boson, the effect of the Higgs diagrams is dominated by the interference contribution and the cross section in the off-peak region $M_T > 130$ GeV is reduced. Under the full set of ATLAS cuts this effect is very small, at the level of 3% of the cross section in the peak region. The effect becomes larger as the $m_{\ell\ell}$ and $\Delta\phi_{\ell\ell}$ cuts are removed, resulting in a sizeable 11% effect in the case of the basic cuts. For comparison, in Table IV we show the expected background cross section from the $q\bar{q}$ process. The background is calculated at lowest order to agree with the treatment of the gg process. The results for the background are shown for the full, basic and basic + $\Delta\phi_{\ell\ell}$ constraint in the three regions of transverse mass considered. The efficacy of the various cuts is a delicate balance between maximizing the signal to background ratio and maintaining a sufficient number of signal events.

In Table V we show the expected cross sections, under the same set of cuts, at $\sqrt{s} = 13$ TeV. At this higher operating energy the value of the peak cross section approximately doubles while the off-peak region grows by a factor of three or more. This is due to the growth of the gluon pdf at small x, to which the tails of the M_T distribution are more sensitive. The relative enhancement of the off-peak region suggests that the types of analyses that we describe in this paper will be more effective at $\sqrt{s} = 13$ TeV.

We now consider varying the Higgs boson width and couplings such that the cross section under the on-shell peak remains constant. The Higgs cross section at 8 TeV has the following form for the case of the full set of cuts:

$$\sigma^{H+I}_{\text{full}} = 5.04 + 0.0395\left(\frac{\Gamma_H}{\Gamma_H^{\text{SM}}}\right)\left(1\text{–}6.41\sqrt{\frac{\Gamma_H^{\text{SM}}}{\Gamma_H}}\right) \text{ fb}. \quad (5)$$

Note that, unlike in the ZZ case, the constants appearing in front of the Γ_H-dependent terms in Eq. (5) cannot simply be inferred from the results given in Table III. This is due to the fact that M_T is only a proxy for the actual quantity that appears in the Higgs boson propagator, s_H. However the functional form of the equation is the same and so we have obtained Eq. (5) by fitting the cross section as a function of Γ_H. Turning to the basic set of cuts the cross section can be parametrized by

$$\sigma^{H+I}_{\text{basic}} = 6.79 + 0.351\left(\frac{\Gamma_H}{\Gamma_H^{\text{SM}}}\right)\left(1\text{–}3.33\sqrt{\frac{\Gamma_H^{\text{SM}}}{\Gamma_H}}\right) \text{ fb}. \quad (6)$$

The impact of the $m_{\ell\ell}$ and $\phi_{\ell\ell}$ cuts is clear from the above equations. The application of these cuts leaves around 75%

of the resonant (NWA) cross section, compared to only 20% and 10% of the interference and off-shell cross sections, respectively. This should be taken into consideration when designing future analyses to be maximally sensitive to the rescaling parameter ξ. In addition it is clear that the interference plays a very important role in these analyses. For values of ξ close to the Standard Model it is the dominant effect and the expected number of Higgs events is reduced. For very large ξ the linear term is most important and the net effect is an increase in the number of Higgs events expected. For the basic set of cuts, Eq. (6) shows that this crossover occurs for $\Gamma_H = 10\Gamma_H^{\rm SM}$.

III. BOUNDING THE HIGGS WIDTH USING ATLAS *WW* DATA

In this section we use the ATLAS $H \to WW$ analysis of Ref. [20] to constrain the Higgs width. This channel is significantly more challenging than the equivalent analysis for $H \to ZZ$. The existing experimental analyses are tailored to a search for on-shell Higgs boson events and only limited information is available regarding the region at high transverse mass which is most sensitive to the Higgs boson width. Therefore our results should only be viewed as indicative of those that may be obtained using a dedicated experimental analysis, which we aim to motivate with this study.

For simplicity we shall use only the 20 fb^{-1} of data taken at 8 TeV and concentrate on the $e\mu + \mu e$ channel, corresponding to the cuts applied in the previous section. The ATLAS collaboration presents results for the expected and observed number of events, including statistical uncertainties, with the fiducial cuts applied sequentially. For the $N_{\rm jet} = 0$ case in which we are interested, the search for the Higgs boson is then performed in the transverse mass window, $0.75m_H < m_T < m_H$. In this fiducial region ATLAS presents a full uncertainty analysis, accounting for a range of systematic effects. For our analysis we wish to be sensitive to off-shell Higgs events so we are primarily interested in the data outside this m_T window. To proceed we must therefore estimate the systematic uncertainty in the wider data set.

We first consider the uncertainty on the background estimate. We expect that a large uncertainty in the $N_{\rm jet} = 0$ bin should come from the normalization of the *WW* background. In their paper ATLAS present a total uncertainty on this quantity that is derived in a control region which is similar to our basic set of cuts. We adopt this uncertainty, 7.4% as one measure of the systematic uncertainty on the expected background (δ_B), ignoring differences in uncertainties associated with subdominant backgrounds and other systematic effects. To account for this oversimplification we also consider the more conservative choices $\delta_B = 10\%$ and $\delta_B = 12\%$. The systematic uncertainty on the signal is dominated by the theory uncertainty and can be inferred from the detailed discussion in Ref. [20], $\delta_S = 21\%$.

Under the assumption $\delta_B = 7.4\%$ we can thus estimate the absolute systematic uncertainty,

$$N^B_{\rm full}({\rm exp}) = 1240 \pm 92, \qquad N^B_{\rm basic}({\rm exp}) = 5490 \pm 406,$$

where we have read off the expected number of events under the full and basic set of cuts from Table 8 of Ref. [20]. For the expected number of signal events we simply rescale our Eqs. (5) and (6) so that the result matches the ATLAS expectation where, for consistency, the effect of the interference is neglected. We thus find

$$N^{H+I}_{\rm full}({\rm exp}) = 118.1 + 0.925\left(\frac{\Gamma_H}{\Gamma_H^{\rm SM}}\right)\left(1 - 6.41\sqrt{\frac{\Gamma_H^{\rm SM}}{\Gamma_H}}\right).$$

for the full set of cuts and, for the basic cuts,

$$N^{H+I}_{\rm basic}({\rm exp}) = 148.3 + 7.67\left(\frac{\Gamma_H}{\Gamma_H^{\rm SM}}\right)\left(1 - 3.33\sqrt{\frac{\Gamma_H^{\rm SM}}{\Gamma_H}}\right).$$

These expectations can then be used to constrain the width of the Higgs boson given that 1399 (full cuts) and 5497 (basic cuts) events were observed in the data. Our results are summarized in Fig. 4, in which we also illustrate the sensitivity to the experimental systematics by plotting results for $\delta_B = 10\%$ and $\delta_B = 12\%$. Note that we have not considered the statistical uncertainty since it is small enough that it has a negligible effect on the final results. We can estimate the theoretical uncertainty by simply considering the uncertainty on the signal expectation discussed above. Using $\delta_B = 7.4\%$ and a 2σ excursion on the expected number of events we find, using the full cuts,

$$\Gamma_H < 365^{+118}_{-79}\Gamma_H^{\rm SM} \tag{7}$$

at 95% confidence. From the discussion of the previous section we expect the limits obtained using the basic cuts to be much more sensitive to the width. Indeed we find

$$\Gamma_H < 125^{+23}_{-22}\Gamma_H^{\rm SM}, \tag{8}$$

although this is also partly driven by the fact that the observed number of events is very close to that expected from background alone. The limit obtained above is around a factor of three weaker than that obtained using a similar analysis of *ZZ* data [17].

In order to increase the sensitivity to a rescaling of the Higgs boson width, it is crucial to focus on the events at large transverse mass. With that in mind we now consider an analysis that uses the basic ATLAS selection cuts

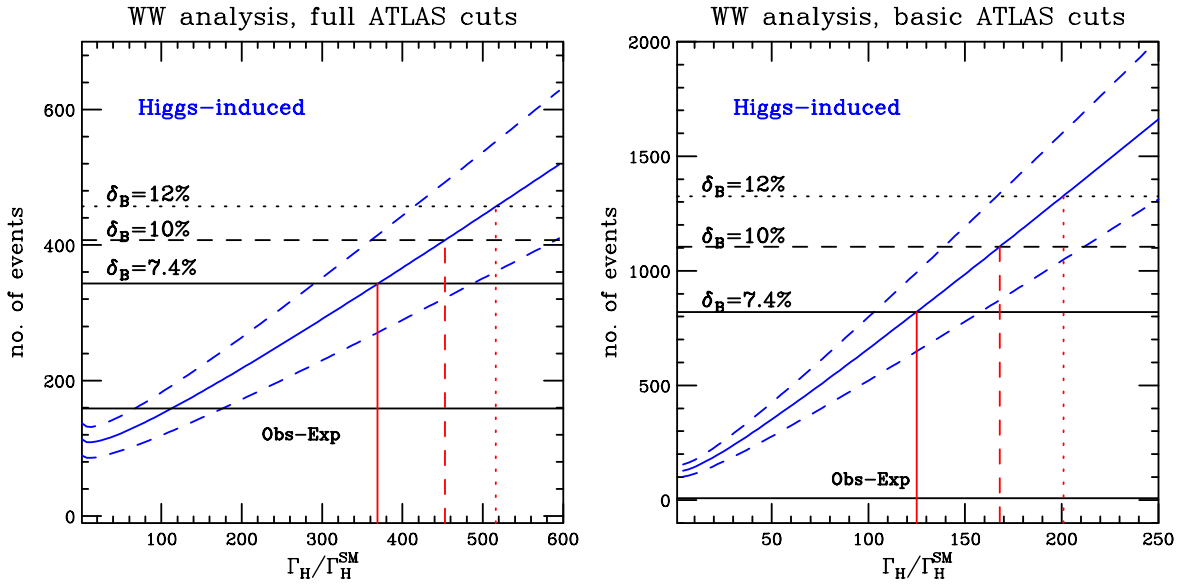

FIG. 4 (color online). Limits on the Higgs width obtained using the results reported by ATLAS. The solid line represents the limit obtained using an estimate of the systematic uncertainty obtained from the results presented in Ref. [20] ($\delta_B = 7.4\%$). The dashed and dotted lines represent limits obtained using the more conservative choices $\delta_B = 10\%$ (dashed) and $\delta_B = 12\%$ (dotted).

defined above but adds a simple transverse mass cut, $M_T > 300$ GeV. Under these cuts the Higgs-induced cross section is

$$\sigma^{H+I}_{M_T} = 0.004 + 0.241\left(\frac{\Gamma_H}{\Gamma_H^{\rm SM}}\right)\left(1\text{–}2.32\sqrt{\frac{\Gamma_H^{\rm SM}}{\Gamma_H}}\right)\ \text{fb}. \qquad (9)$$

To obtain the expected number of signal events in the high-M_T region, we simply rescale this cross section by the same factor that is necessary to obtain the ATLAS expectation in the whole M_T range, i.e., the factor that was used for the basic cuts previously. In order to estimate the expected number of background events we compute the fraction of the continuum WW background process that survives the $M_T > 300$ GeV cut at leading order. This fraction is around 6% and leads to an estimate of 336 background events. Rather than extrapolating our assumed background uncertainty from the previous analysis, we simply present estimates of the expected limits that would be obtained with $\delta_B = 5, 10, 15\%$. We maintain the same theoretical uncertainty (21%) on the Higgs signal. Our results are summarized in Fig. 5. As expected the large M_T region is more sensitive to the Higgs width rescaling. For instance, the expected 95% confidence limit for $\delta_B = 10\%$ is

$$\Gamma_H < 45^{+9}_{-7}\Gamma_H^{\rm SM}. \qquad (10)$$

In comparison, the result from using a similar analysis in the ZZ channel with $m_{4\ell} > 300$ GeV is around $25\Gamma_H^{\rm SM}$ [16,17]. These results suggest that if the total experimental uncertainty can be constrained to below 10%, then the WW results can be complementary to, and even competitive with, those found in the ZZ mode. Finally, we note that it is possible that the limits in the WW channel could be further improved by including the ee and $\mu\mu$ results. However, the

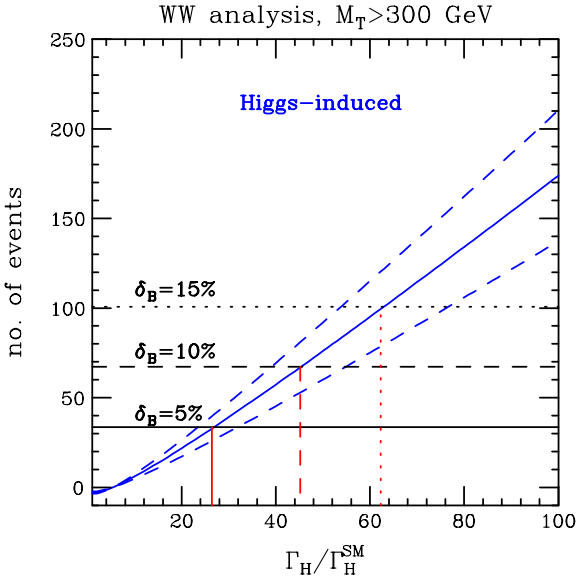

FIG. 5 (color online). Estimated limits on the Higgs width obtained using a cut on the transverse mass, $M_T > 300$ GeV. The limits are computed using an estimate of the expected background cross section, as described in the text, and for different projected experimental uncertainties. The number of signal events is also estimated from the ATLAS 20 fb^{-1} expectation, with the corresponding theoretical uncertainty represented by the dashed curves.

analysis is already dominated by systematic uncertainties, so that limits obtained by including this data should not be significantly better than those suggested here.

IV. CONCLUSIONS

In this paper we have motivated the use of existing LHC data to bound the Higgs width, using off-shell Higgs events in the WW final state. The analysis proceeds in a similar fashion to the ZZ channel [16,17]. The essential idea is that the cross section depends on the width of the Higgs boson in different ways near the peak region and away from it. This technique is optimal in instances in which one can directly measure the four-momentum squared of the Higgs boson, s_H, thus allowing for a clean separation of the two regions of phase space. In decays such as $H \to WW \to 2\ell 2\nu$ this is impossible due to the presence of neutrinos that are identified only as missing transverse momentum. However in these decays the transverse mass M_T acts as an appropriate proxy for $\sqrt{s_H}$. The narrow peak in $\sqrt{s_H}$ is transformed into a broad excess in M_T, but the kinematics of the decay result in an edge at $M_T = m_H$. As a result there are very few on-shell events in the $M_T > m_H$ region.

Using 20 fb^{-1} of 8 TeV ATLAS $e\mu + \mu e$ data we investigated the potential for constraints on the Higgs width now and in the future. Since the existing analysis is dedicated to the search for, and measurement of, on-shell Higgs events, the current cuts are not ideal for our purpose. Nevertheless we estimate a bound on the Higgs width at approximately 125 times the SM value. We illustrated how these limits could be significantly improved by focusing on the region of high transverse mass. If an experimental precision corresponding to a background uncertainty of $\delta_B \lesssim 10\%$ could be achieved then the existing data may be able to bound the Higgs width at the level of $(25\text{–}50)\Gamma_H^{\rm SM}$. For this reason we believe that a full experimental analysis, focusing particularly on the high-M_T region of the $N_{\rm jet} = 0$ bin of the WW channel, is extremely well motivated.

ACKNOWLEDGMENTS

The research of R. K. E. and J. M. C. is supported by the U. S. DOE under Contract No. DE-AC02-07CH11359.

[1] G. Aad *et al.* (ATLAS Collaboration), Phys. Lett. B **716**, 1 (2012).
[2] S. Chatrchyan *et al.*(CMS Collaboration), Phys. Lett. B **716**, 30 (2012).
[3] ATLAS Collaboration, Report No. ATLAS-COM-CONF-2013-025 (2013).
[4] S. Chatrchyan *et al.* (CMS Collaboration), Phys. Rev. Lett. **110**, 081803 (2013).
[5] G. Aad *et al.* (ATLAS Collaboration), Phys. Lett. B **726**, 120 (2013).
[6] G. Aad *et al.* (ATLAS Collaboration), Phys. Lett. B **726**, 88 (2013).
[7] CMS Collaboration, Report No. CMS-PAS-HIG-13-005 (2013).
[8] T. Han, Z. Liu, and J. Sayre, arXiv:1311.7155.
[9] T. Han and Z. Liu, Phys. Rev. D **87**, 033007 (2013).
[10] A. Conway and H. Wenzel, arXiv:1304.5270.
[11] B. A. Dobrescu and J. D. Lykken, J. High Energy Phys. 02 (2013) 073.
[12] L. J. Dixon and Y. Li, Phys. Rev. Lett. **111**, 111802 (2013).
[13] L. J. Dixon and M. S. Siu, Phys. Rev. Lett. **90**, 252001 (2003).
[14] S. P. Martin, Phys. Rev. D **86**, 073016 (2012).
[15] S. P. Martin, Phys. Rev. D **88**, 013004 (2013).
[16] F. Caola and K. Melnikov, Phys. Rev. D **88**, 054024 (2013).
[17] J. M. Campbell, R. K. Ellis, and C. Williams, arXiv:1311.3589.
[18] V. Barger, T. Han, and J. Ohnemus, Phys. Rev. D **37**, 1174 (1988).
[19] A. J. Barr, B. Gripaios, and C. G. Lester, J. High Energy Phys. 07 (2009) 072.
[20] ATLAS Collaboration, Report No. ATLAS-CONF-2013-030 (2013).
[21] CMS Collaboration, Report No. CMS-PAS-HIG-12-042 (2012).
[22] S. Chatrchyan *et al.* (CMS Collaboration), J. High Energy Phys. 01 (2014) 096.
[23] D. A. Dicus, C. Kao, and W. Repko, Phys. Rev. D **36**, 1570 (1987).
[24] E. N. Glover and J. van der Bij, Phys. Lett. B **219**, 488 (1989).
[25] T. Binoth, M. Ciccolini, N. Kauer, and M. Kramer, J. High Energy Phys. 03 (2005) 065.
[26] T. Binoth, M. Ciccolini, N. Kauer, and M. Kramer, J. High Energy Phys. 12 (2006) 046.
[27] J. M. Campbell, R. K. Ellis, and C. Williams, J. High Energy Phys. 07 (2011) 018.
[28] Z. Bern, L. J. Dixon, and D. A. Kosower, Nucl. Phys. **B513**, 3 (1998).
[29] J. M. Campbell, R. K. Ellis, and C. Williams, J. High Energy Phys. 10 (2011) 005.
[30] N. Kauer and G. Passarino, J. High Energy Phys. 08 (2012) 116.
[31] N. Kauer, arXiv:1310.7011.
[32] M. Bonvini, F. Caola, S. Forte, K. Melnikov, and G. Ridolfi, Phys. Rev. D **88**, 034032 (2013).
[33] A. Martin, W. Stirling, R. Thorne, and G. Watt, Eur. Phys. J. C **63**, 189 (2009).